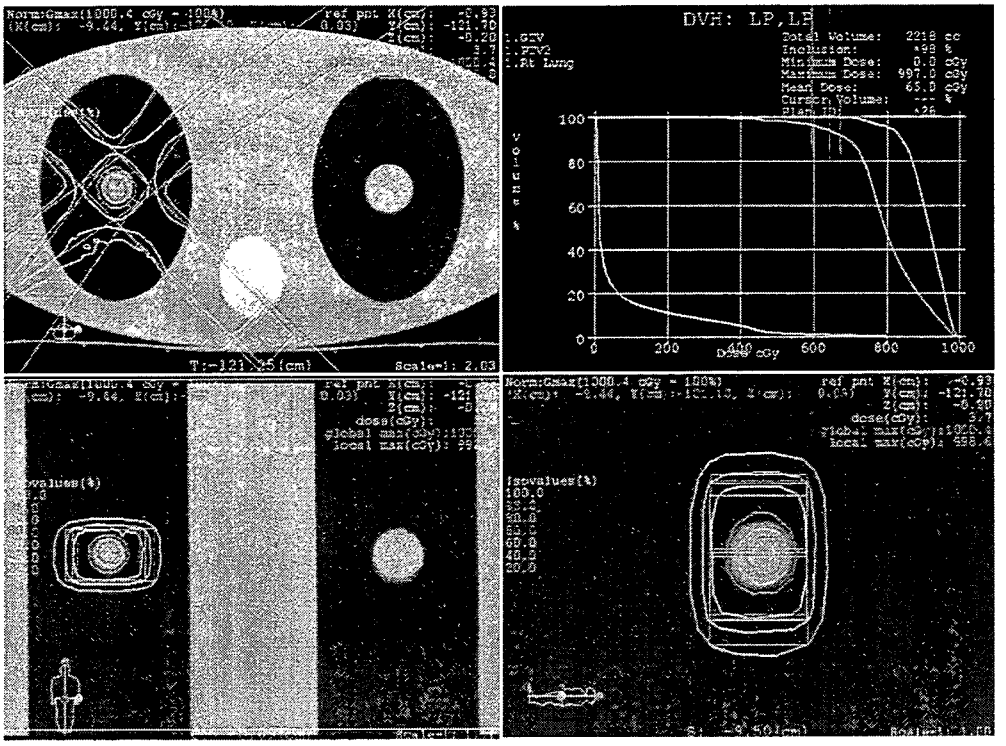

Fig. 2. Display of the Monte Carlo dose on the XiO RTP system. A 6-MV photon beam was used to calculate the MC dose using CT data from a thorax phantom. *Top left*, axial view of the isocenter slice; *top right*, dose-volume histograms of the gross tumor volume (GTV), planning tumor volume (PTV), and right lung; *bottom left*, coronal view; *bottom right*, sagittal view. The target was in the right lung; it was 2 cm in diameter, which was defined as the GTV. A 5-mm margin around the GTV was considered the PTV. A four-field plan was generated, and symmetrical 3 × 3 cm beams were applied to cover the target volume

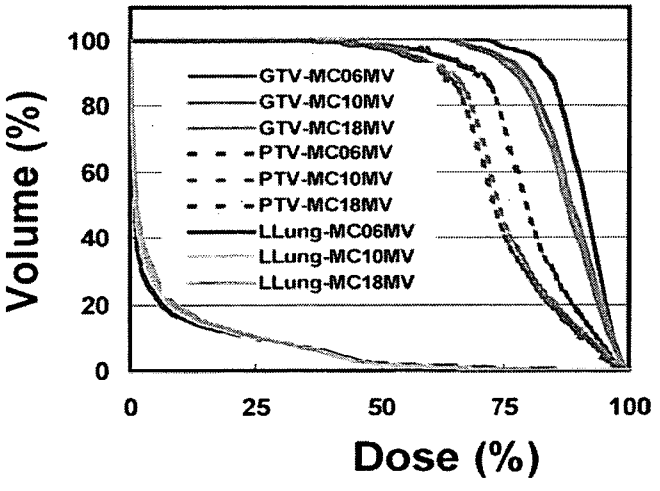

Fig. 3. Dose-volume histograms of Monte Carlo doses for 6-, 10-, and 18-MV photon beams calculated using the CT data of a thorax phantom. The diameter of the GTV was 2 cm, the PTV was GTV + 0.5 mm, and the applied beam size was 3 × 3 cm

the companion code DOSXYZnrc[3] performs particle transport in a rectilinear voxel geometry and can be used for the simulation of patient irradiation. All dose calculations in this work for kVp and MV energies were performed using phase space files calculated and stored previously.[8,9] Although a phase space file is inconvenient to handle owing to its large size, it gives the most accurate dose results.[3] Therefore, this was the method used in this study.

As it is important to evaluate MC dose distributions in defined anatomical CT structures in the form of DVHs, some tools based on the MATLAB environment have already been developed.[16,17] This toolbox supports DICOM (Digital Imaging and Communication in Medicine) radiotherapy extension (DICOM-RT)[16,17] or RTOG (Radiation Therapy Oncology Group, respectively)[16] formats to import the plan from the RTP system and allows analysis of the three-dimensional (3D) RTP dose for RTP dose plan verifications. The toolbox provides an independent platform for 3D dose data analysis and the capability to analyze MC dose data.

In this study, we have developed the interface to convert the MC dose file format to XiO dose file format and to export the MC dose to the XiO RTP planning system for display and quantitative analyses. It is keyboard-interactive software, and its operation is simple. Once the conversion is performed, the result of the MC dose calculation can be treated in the same manner as the usual XiO manipulation. The interface software is based on the Linux environment and is written in the C++ language; it does not require any commercial software for XiO users. The developed toolbox/software can be requested from the authors. Although the current version is compatible with XiO 4.2, we are planning to upgrade the interface for version 4.3 of XiO.

BEAMnrc and its associated code DOSXYZnrc are extensively used in radiotherapy research. Three-dimensional display of DOSXYZnrc dose on a dedicated RTP

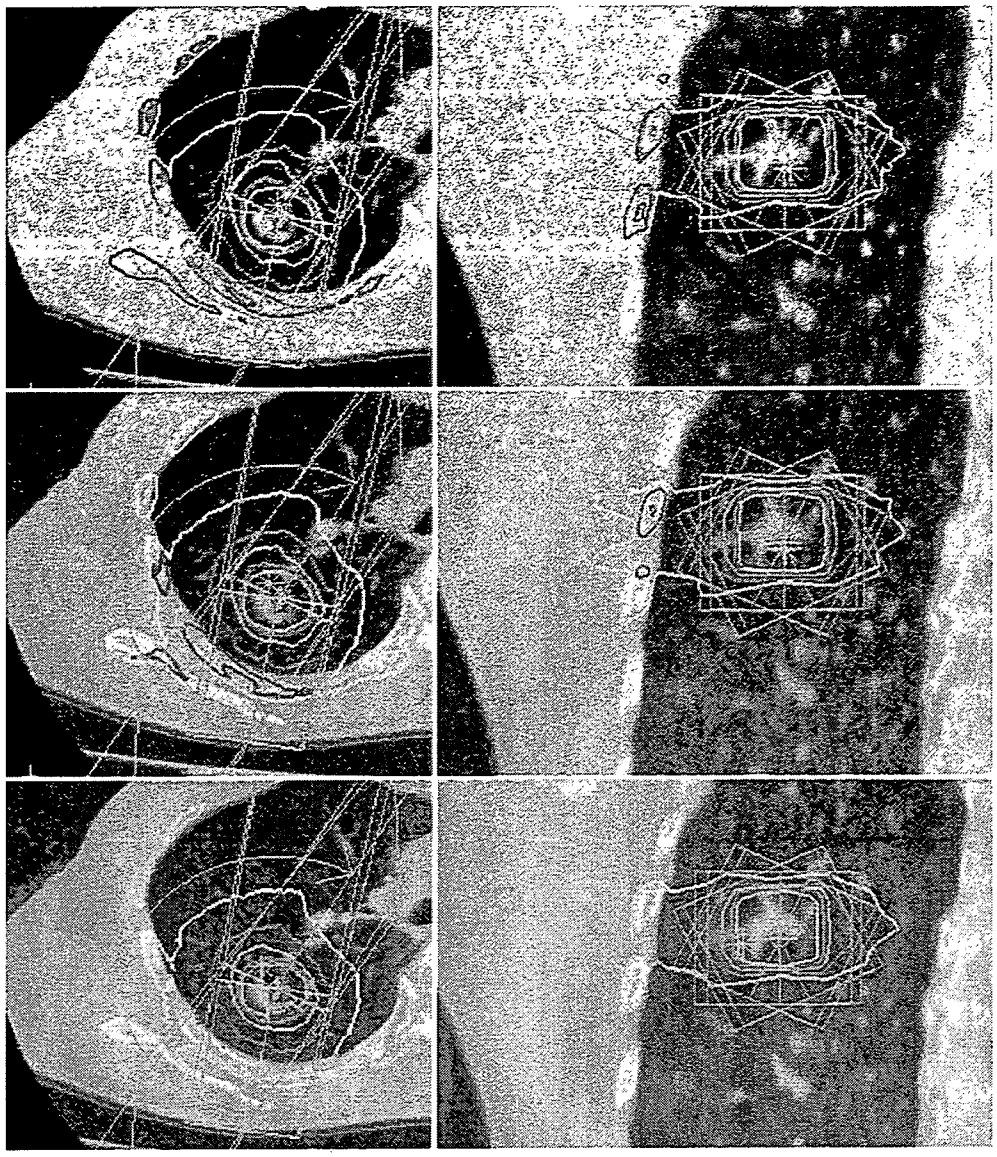

Fig. 4. Monte Carlo dose calculated for a human lung tumor for X-ray energies of 200 kVp (*top panels*), 300 kVp (*middle panels*), and 500 kVp (*bottom panels*). Dose distributions on the axial images (isocenter slice) and coronal images displayed with the XiO RTP system are shown in the figure with the beam arrangement. In all cases, doses were normalized with the isocenter dose within the GTV. Isodose lines with orange, red, green, blue, and yellow colors indicate 95%, 80%, 60%, 40%, and 20% of the isocenter dose, respectively

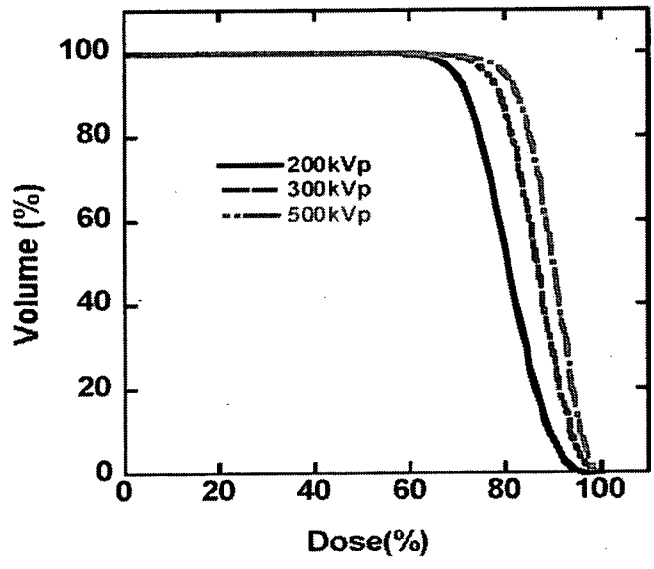

Fig. 5. Monte Carlo dose-volume histogram of the target, with the GTV dose calculated for a human lung tumor with X-ray energies of 200, 300, and 500 kVp. In all cases, doses were normalized with the isocenter dose within the GTV

system can provide all the existing facilities of the system for quantitative dose analysis. The interface we have developed to display the 3DCRT DOSXYZnrc MC dose on the XiO RTP system is an excellent tool, and all the facilities of the XiO RTP system can be used for quantitative evaluation of doses such as DVH on a defined structure.

Acknowledgments. This research is part of the IMAGINE project supported by the Japan Science and Technology (JST) CREST program. We are thankful to CMS Japan for their technical support.

References

1. Rogers DW, Faddegon BA, Ding GX, Ma CM, We J, Mackie TR. BEAM: a Monte Carlo code to simulate radiotherapy treatment units. Med Phys 1995;22:503–24.
2. Nelson WR, Hirayama H, Rogers DW. The EGS4 code system. In: Report SLAC-265. Stanford, CA: Stanford Linear Accelerator Center; 1985.
3. Walters BRB, Rogers DW. DOSXYZnrc users manual. In: NRSS report RIRS-794. Ottawa: NRSS; 2002.
4. Kawrakow I, Rogers DW. The EGSnrc code system: Monte Carlo simulation of electron and photon transport. In: Technical report PIRS-701. Ottawa: NRCC; 2000.
5. Kawrakow I. The dose visualization tool dosxyz_show. In: Dose visualization tool dosxyz_show. Ottawa: National Research Council of Canada; 1998.
6. ICRU. Report 50: Prescribing, recording and reporting photon beam therapy. Washington, DC: International Commission on Radiation Units and Measurements; 1993.
7. ICRU. Report 62: Prescribing, recording and reporting photon beam therapy (supplement to ICRU report 50). Bethesda, MD: International Commission on Radiation Units and Measurements; 1999.
8. Deloar HM, Griffin J, Bird M, Wilder B, Morgan S, Hsieh W-I, et al. Evaluation of clinical dose distributions using Monte Carlo methods. In: The World Congress on medical physics and biomedical engineering. Seoul: Springer; 2006; p. 1840–1.
9. Deloar HM, Kunieda E, Kawase T, Saitoh H, Ozaki M, Fujisaki T, et al. Monte Carlo simulations for stereotactic radiotherapy system with various kilo voltage X-ray energy. In: 3rd International EGS workshop. Tsukuba, Ibaraki, Japan: KEK (High Energy Accelerator Research Organization); 2004.
10. Mackie TR, Ahnesj A, Dickof P, Snider A. Development of a convolution/superposition method for photon beams. In: 9th International conference on computers in radiotherapy, Amsterdam, 1987.
11. Miften M, Wiesmeyer M, Monthofer S, Krippner K. Implementation of FFT convolution and multigrid superposition models in the FOCUS RTP system. Phys Med Biol 2000;45: 817–33.
12. Lovelock DM, Chui CS, Mohan R. A Monte Carlo model of photon beams used in radiation therapy. Med Phys 1995;22: 1387–94.
13. Ma CM, Jiang SB. Monte Carlo modelling of electron beams from medical accelerators. Phys Med Biol 1999;44:R157–89.
14. Mohan R, Chui C, Lidofsky L. Energy and angular distributions of photons from medical linear accelerators. Med Phys 1985:12:592–7.
15. Shortt KR, Ross CK, Bielajew AF, Rogers DW. Electron beam dose distributions near standard inhomogeneities. Phys Med Biol 1986;31:235–49.
16. Deasy JO, Blanco AI, Clark VH. CERR: a computational environment for radiotherapy research. Med Phys 2003;30: 979–85.
17. Spezi E, Lewis DG, Smith CW. A DICOM-RT-based toolbox for the evaluation and verification of radiotherapy plans. Phys Med Biol 2002;47:4223–32.

甲状腺分化癌　治療

甲状腺疾患に対する放射線外照射

茂松直之[1]　奥　洋平[1]　国枝悦夫[1]
久保敦司[1]　高見　博[2]

External radiation therapy for thyroid disease

[1]Naoyuki Shigematsu, [1]Youhei Oku, [1]Etsuo Kunieda,
[1]Atsushi Kubo, [2]Hiroshi Takami
[1]Department of Radiology, Keio University, School of Medicine
[2]Department of Surgery, Teikyo University, School of Medicine

Abstract

The external beam irradiation plays a very important role in the treatment of some thyroid diseases, such as primary cancers (papillary, follicular, medullary and anaplastic), malignant lymphoma and bone metastasis. The treatment policies, the irradiation techniques and the treatment results of these diseases are described from our experiences and the literature. The recent improvements of irradiation techniques are also explained.

Key words: external irradiation, thyroid cancer, malignant lymphoma, bone metastasis

はじめに

甲状腺疾患において放射線の外照射を適応する疾患としては，甲状腺癌(乳頭癌・濾胞癌・髄様癌・未分化癌)，悪性リンパ腫，甲状腺癌の骨転移などがあげられる．これらの病態における治療方針，照射方法および治療成績に関し文献的考察を行うとともに，最近の外照射方法の進歩に関して説明する．

1. 乳頭癌・濾胞癌

a. 治療方針

乳頭癌・濾胞癌は基本的には放射線感受性は低く，通常の放射線外照射でコントロールすることは期待できず，治療法の第一選択は外科的切除である．ただし原発巣の切除範囲およびリンパ節の郭清範囲は，我が国と海外では大きく異なる[1]．海外では腫瘍の大きさにかかわらず甲状腺全摘が標準で，リンパ節の郭清範囲は狭い．これに対して我が国では甲状腺の切除範囲は小さく，正常甲状腺を温存する手術が多く行われ，一方でリンパ節の郭清範囲は広範囲に及ぶ(図1)．海外では甲状腺は全摘し，残存・転移病巣は^{131}I内用療法を積極的に行うことが前提にあるのに対し，我が国では術後も甲状腺機能を維持し手術のみで根治を狙うというポリシーの違いがある．術後のQOL(quality of life)，経過観察様式，補助療法，再発後の治療などに関しそれぞれメリット・デメリットがあり[2]，比較的予後の良好な分化癌においてその優劣は簡単には決められないが，我が国では世界的にみると独特な治療方針が選択されているということはできる．

しかしながら，手術が第一選択であることに

[1]慶應義塾大学医学部放射線科　[2]帝京大学医学部外科

0047-1852/07/¥40/頁/JCLS

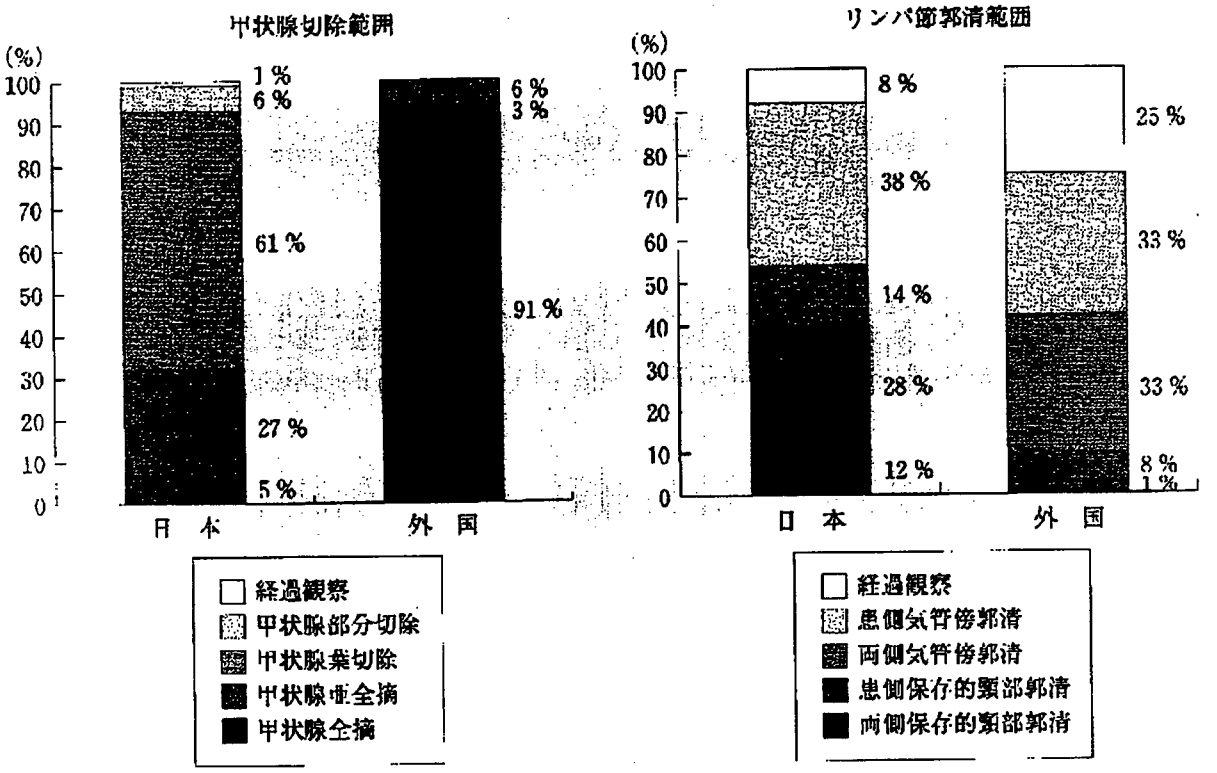

図1　分化癌(1-2cm)における甲状腺切除範囲とリンパ節郭清範囲の我が国と海外の比較

は違いはなく，術後の再発の場合も再手術による可及的な切除が行われることが多い．甲状腺が全摘された後の残存腫瘍で手術の適応がない場合，あるいは転移腫瘍では，^{131}I内用療法が考慮され，その効果も期待できる．一方ヨード摂取能のない腫瘍の場合はその適応はなく，ここで放射線外照射の適応が考慮される．海外での放射線外照射の適応は術後残存病変，術後再発予防(甲状腺外浸潤・リンパ節転移例)，手術不能例，局所再発でヨード摂取能のない場合，^{131}I治療後の再発[3,11]とされている．転移病巣に対する適応は後述する．

前述のように基本的には放射線感受性は低い腫瘍であり，^{131}I内用療法のように高線量が投与できない放射線外照射が有効な適応症例は少ない．また，外照射は正常組織の合併症を考慮すると一部位に関しては1回の適応が原則なので(再照射は不能)，外照射をどの段階で施行するかに関しては十分な検討が必要である．

b. 照射方法

術後の外照射の範囲と線量は，リンパ節転移陰性であれば甲状腺床とその辺縁2cm程度の範囲を含めて1回2Gyで計60-70Gy，リンパ節転移陽性であれば(その転移範囲にもよるが)，頸部-上縦隔リンパ節領域を広範囲に1回2Gy

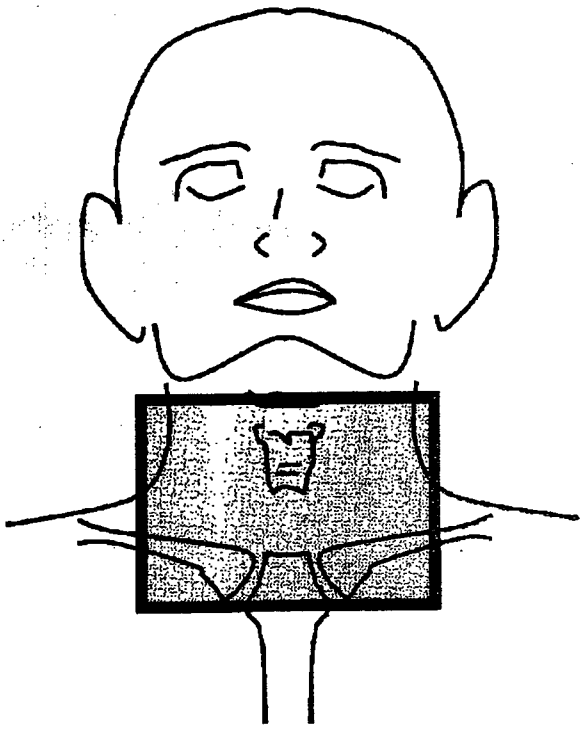

図2　甲状腺に対する限局型照射野

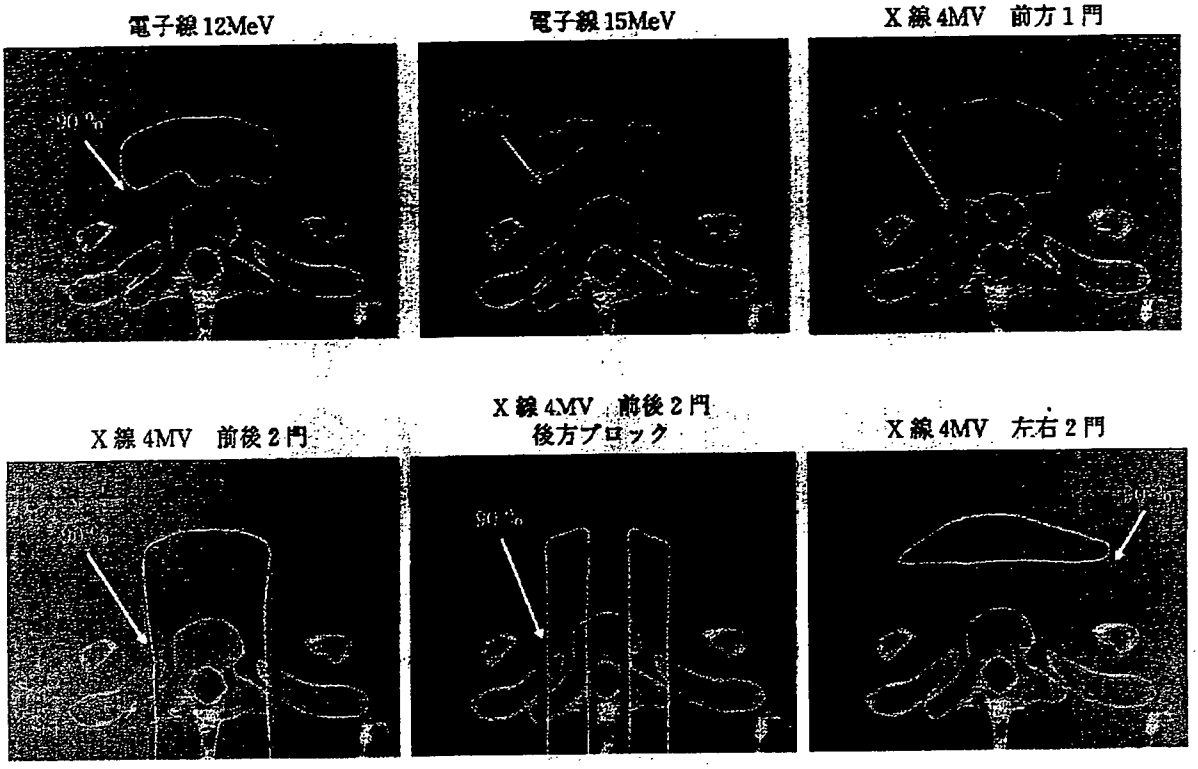

図3 各種放射線による限局型照射の線量分布

で40-50 Gy照射後，甲状腺局所に10-20 Gy追加する[6]．

照射の詳細に関しても施設ごとに異なるが，電子線(12，15 MeV)による前方1門照射，X線による前方1門照射，前後2門照射，左右2門照射などの選択肢がある．個々の症例で放射線の線量分布図を作成し，甲状腺に適切な照射がなされ，食道や脊髄などの正常組織に過線量の照射が行われないように適切な照射方法を選択することが重要である．

リンパ節転移陰性であれば**図2**のような範囲の甲状腺床に対する外照射野を計画する．この際，電子線かX線か，またエネルギーや照射法により線量分布が異なり，DVH(dose volume histogram)解析にてその有用性を判断しなければならない．仮想で作成した様々な照射法における線量分布(**図3**)とDVH解析(**図4**)を示したが，個々の症例でこのような検討を行い適切な照射方法を決定しなければならない．

リンパ節転移陽性であれば**図5**のような範囲の外照射野が推奨される．X線が使用されるが，やはり照射法により線量分布が異なり，DVH解析にてその有用性を判断しなければならない．仮想で作成した様々な照射法における線量分布とDVH解析を示した(**図6**)．

c. 治療成績

放射線外照射の適応の可否に関するランドマイズドトライアルは残念ながら存在しないが，照射群で局所制御率が上昇したとする報告は多く[5,9]，また10年生存率改善の報告も幾つか認められる[8,9]．**図7**にその報告例を示した．

2. 髄 様 癌

a. 治療方針

髄様癌も治療の主体は手術による切除であり，術後の残存病変あるいは手術不能例が放射線外照射の適応となるが，乳頭癌・濾胞癌と同様に放射線感受性は低く，外照射の有用性に関してはいまだ議論の多いところである[10]．

b. 照射方法

乳頭癌・濾胞癌と比較してリンパ節転移の頻度が高率であり，外照射は頸部-上縦隔リンパ節領域を広範囲に，1回2 Gyで40-50 Gy照射後，甲状腺局所に10-20 Gy追加する[10,11](**図5**)．

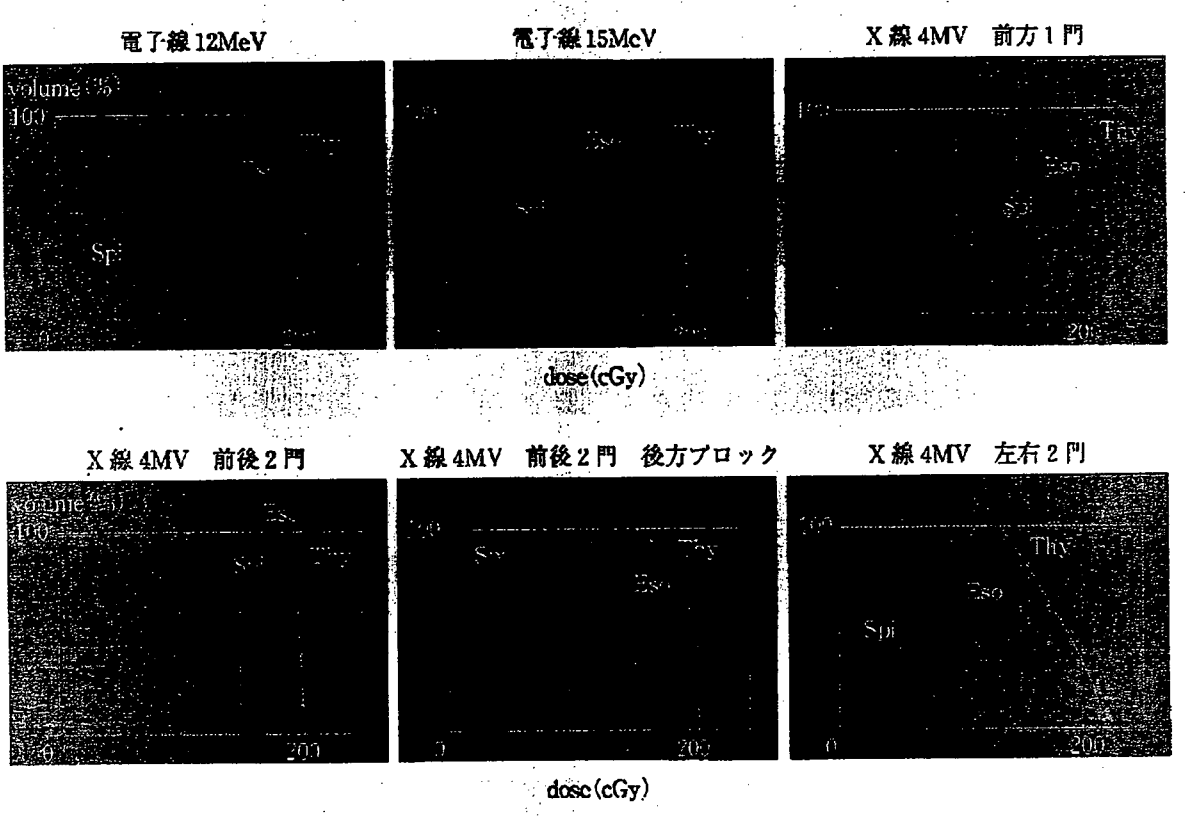

図4 各種放射線による限局型照射のDVH解析
Thy: thyroid, Eso: esophagus, Spi: spinal cord.

c. 治療成績

放射線外照射の適応の可否に関するランドマイズドトライアルは残念ながら存在しない．放射線外照射の効果は期待できず，照射野内再発が30%にみられるという報告[12]もあるが，一方で術後顕微鏡的残存・甲状腺外浸潤・リンパ節転移陽性の高危険群では10年局所制御率は外照射群で86%，非照射群で52%(p=0.049)とする報告もある[11]．リンパ節転移に加えて遠隔転移も高頻度に認められ，生存率の改善を示した報告はほとんど認められない．

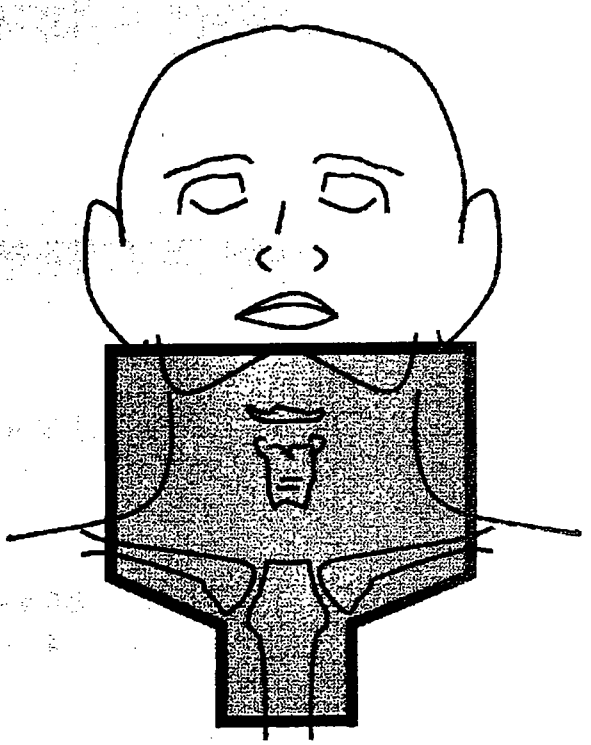

図5 甲状腺に対する広範囲照射野

3. 未分化癌

a. 治療方針

甲状腺癌の中では極めて予後が不良で，急速に増大し高率に遠隔転移を伴う疾患である．根治切除可能例でも局所再発・遠隔転移が高率で，有用な治療法は確立されていないのが現状であるが，極少数の長期生存者のほとんどは，外科的切除・外照射・多剤化学療法併用例であり，

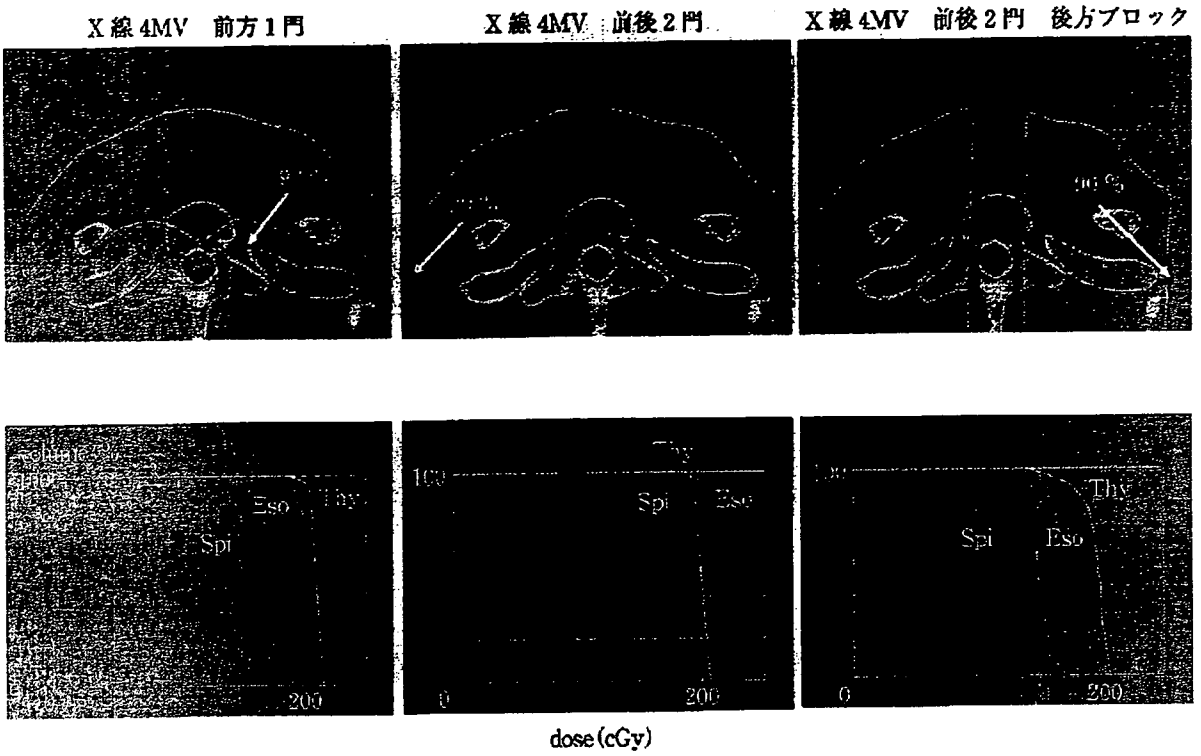

図6 各種放射線による広範囲照射の線量分布(上)とDVH解析(下)
Thy: thyroid, Eso: esophagus, Spi: spinal cord.

集学的な様々な治療が試みられる.

b. 照射方法

外照射は頸部-上縦隔リンパ節領域を広範囲に,1回2Gyで40-50Gy照射後,甲状腺局所に10-20Gy追加する(図5).

c. 治療成績

ランドマイズドトライアルは残念ながらない.集学的治療を行っても治療成績は極めて不良で,2年以上の生存例は5%程度である.放射線の有用性を示した報告はほとんどないが,Kebebewらは生存率は極めて低率であるが,術後の放射線外照射により無病生存率が改善し,多変量解析でも外照射が有意な因子であったと報告している[13].

4. 悪性リンパ腫

a. 治療方針

甲状腺の悪性リンパ腫は他の部位の悪性リンパ腫と同様,局所の浸潤による気道狭窄などの切迫症状がないかぎり外科的切除は不要で,Ann Arbor分類でI-II期であれば,化学療法および放射線療法の良い適応疾患であり,適切な治療が行われれば根治の可能性が高い疾患である.甲状腺は他部位と同様diffuse large B cell lymphoma(DLBL)が多く認められるが,そのなかでmucosa-associated lymphoid tissue(MALT)由来のリンパ腫が比較的多く認められる組織である.

DLBLではCHOP(シクロホスファミド,ドキソルビシン(アドリアマイシン),ビンクリスチン,プレドニゾロン)あるいは,R-CHOP(リツキシマブ+CHOP)を3(-6)コース行い,その後外照射を併用する.MALTリンパ腫でもCHOPと外照射を行う施設もあるが,外照射単独治療でも根治可能との報告もある.

b. 照射方法

外照射は頸部-上縦隔リンパ節領域を広範囲に照射する(図5).DLBLではCHOP施行後,完全寛解であれば1回2Gyで30(-40)Gy,非完全寛解であれば局所に10(-20)Gy追加する.MALTリンパ腫では1回2Gyで30Gy程度の照射を施行する.

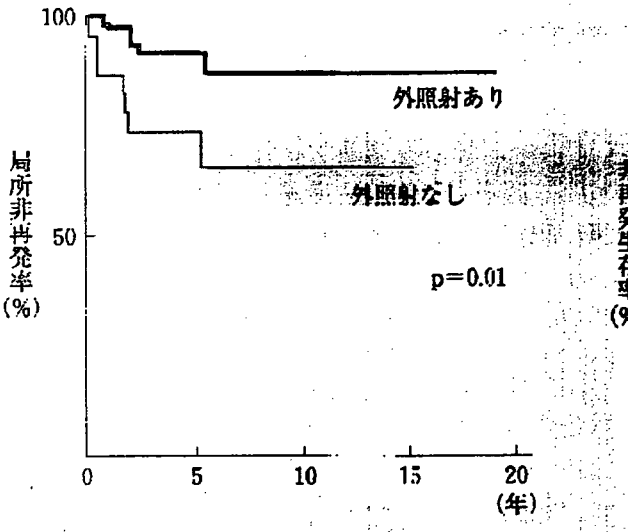

図7 甲状腺外浸潤を認めた分化癌70症例に対する治療成績
術後照射の有無による局所非再発率の比較.
(文献[9]より引用)

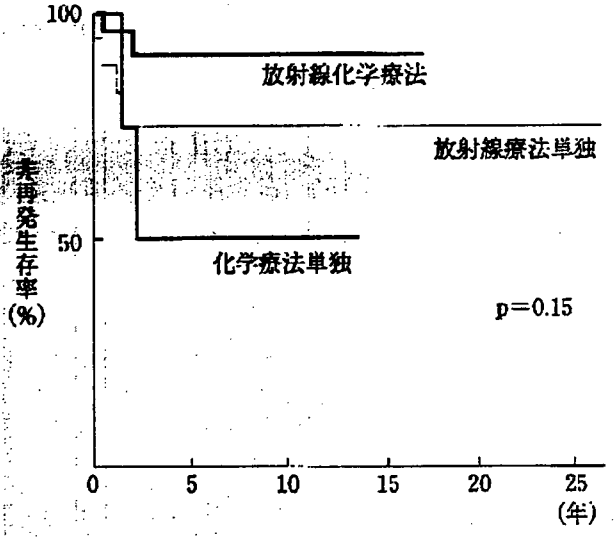

図8 甲状腺悪性リンパ腫(I-II期)の治療成績
放射線治療18例, 化学療法5例および放射線化学療法24例の非再発生存率の比較.
(文献[14]より引用)

c. 治療成績

甲状腺リンパ腫の長期治療成績に関するランドマイズドトライアルはない. DLBLに関して長期に経過観察を行ったHaらの51例の報告があるが様々な治療方針による症例が混在している[14]. 治療成績を図8に示すが, 化学療法と放射線治療の併用療法で非再発率は90%程度である. 甲状腺MALTリンパ腫の報告もほとんど存在しない. Tsangらの報告では放射線治療単独療法を中心とした治療法で13例の症例で5年間で再発症例を認めず[15], 予後は極めて良好と考えられる.

5. 骨 転 移

a. 治療方針

甲状腺の骨転移はその他の臓器転移(肺転移)などと比較すると, すぐに生命予後を脅かすことは少ないが疼痛・病的骨折・神経障害などでQOLを大きく低下させることがある. 治療法としては手術・神経ブロック・放射線治療・鎮痛剤などがあるが, 転移の部位, 数, 症状, 予後などに応じて治療法の選択の判断が重要である. 転移が単発の場合は手術も考慮され, 数カ所(1-3カ所程度)であれば放射線治療, 多発性の場合は鎮痛剤の適応となることが多いが, これらの併用療法も多く行われる.

b. 照射方法

症状(疼痛・神経麻痺)や, 画像診断(単純写真・骨シンチ・CT・MRI・PETなど)を参考にして照射範囲を計画し, 予後を考慮して照射線量と回数を設定する. 数年の長い生命予後が期待される場合は長期の放射線合併症も考慮して1回線量をあまり増大せずに40-50 Gy/20-25回で照射, 長期予後が期待できない場合は30 Gy/10回, 20 Gy/5回などの短期照射を設定する.

c. 治療成績

骨転移への放射線外照射は残念ながら生存率改善に寄与はしないが, 甲状腺癌を含む多くの骨転移による疼痛の80%に鎮痛効果が期待できると報告されている[16].

6. 最近の放射線外照射の進歩

前述のように, 甲状腺癌に対する放射線外照射では通常の方法では, 正常組織の耐容線量による制限から1回2 Gyで60-70 Gyが照射線量の限界で, 放射線感受性の低い甲状腺高分化癌では外照射による治療効果は期待ができなかった. しかしながら近年では最新の放射線治療装置を用いてコンピュータ制御で行う, ごく狭い

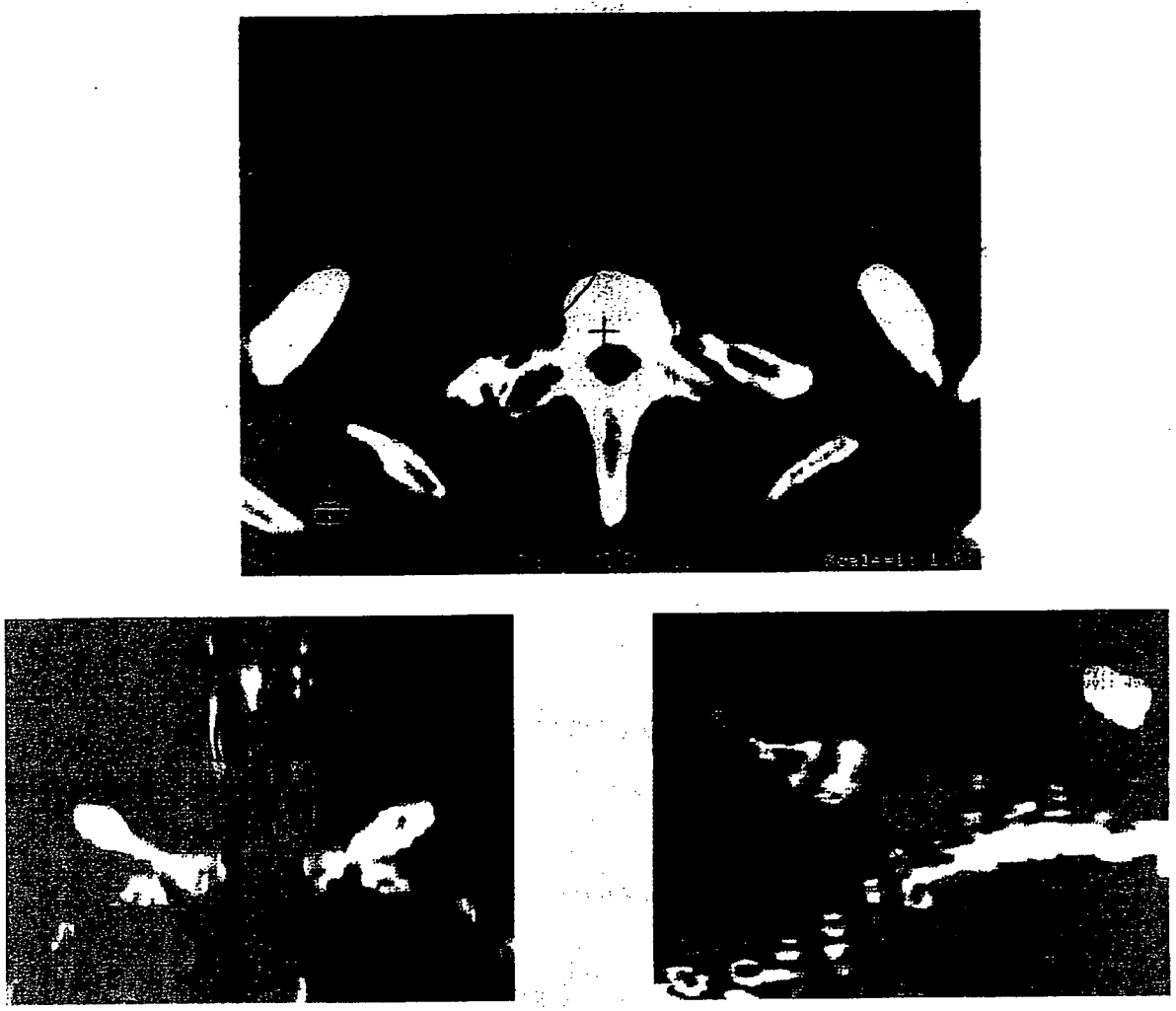

図9 甲状腺に対するSRT計画の一例

範囲に放射線照射線量を集中させる定位的放射線照射(stereotactic radiation therapy: SRT)や，不規則な形状の腫瘍に照射野を設定できる強度変調放射線照射(intensity modulated radiation therapy: IMRT)などが施行可能となり，外照射で局所の線量を増大できる治療法が普及してきている．図9にSRT計画の一例，図10にIMRT計画の一例を示したが，このような治療法により甲状腺の外照射の適応は今後増大していくと期待される．

■文　献

1) 茂松直之ほか：日本および外国での高分化甲状腺癌に対する治療方針の相違—日本甲状腺外科学会と国際内分泌外科学会会員に対するアンケート結果．日医師会誌　135(6)：1333-1340, 2006.
2) Shigematsu N, et al: Unique treatment policy for well-differentiated thyroid cancer in Japan: results of a questionnaire distributed to members of the Japanese Society of Thyroid Surgery and the International Association of Endocrine Surgeons. Endocr J　53: 829-839, 2006.
3) Schlumberger MJ: Papillary and follicular thyroid carcinoma. N Engl J Med　338(5): 297-306, 1998.
4) Brierley JD, et al: External-beam radiation therapy in the treatment of differentiated thyroid cancer. Semin Surg Oncol　16(1): 42-49, 1999.
5) Lin JD, et al: Results of external beam radiotherapy in patients with well differentiated thyroid

図10 甲状腺に対するIMRT計画の一例

carcinoma. Jpn J Clin Oncol 27(4): 244-247, 1997.
6) Kim TH, et al: Value of external irradiation for locally advanced papillary thyroid cancer. Int J Radiat Oncol Biol Phys 55(4): 1006-1012, 2003.
7) Chow SM, et al: Papillary thyroid carcinoma: prognostic factors and the role of radioiodine and external radiotherapy. Int J Radiat Oncol Biol Phys 52(3): 784-795, 2002.
8) Tsang RW, et al: The effects of surgery, radioiodine, and external radiation therapy on the clinical outcome of patients with differentiated thyroid carcinoma. Cancer 82(2): 375-388, 1998.
9) Brierley J, et al: Prognostic factors and the effect of treatment with radioactive iodine and external beam radiation on patients with differentiated thyroid cancer seen at a single institution over 40 years. Clin Endocrinol(Oxf) 63(4): 418-427, 2005.
10) Frank J, et al: Medullary thyroid carcinoma: Including MEN 2A and MEN 2B syndromes. J Surg Oncol 89(3): 122-129, 2005.
11) Brierley J, et al: Medullary thyroid cancer: analyses of survival and prognostic factors and the role of radiation therapy in local control. Thyroid 6(4): 305-310, 1996.
12) Nguyen TD, et al: Results of postoperative radiation therapy in medullary carcinoma of the thyroid: a retrospective study by the French Federation of Cancer Institutes—the Radiotherapy Cooperative Group. Radiother Oncol 23(1): 1-5, 1992.
13) Kebebew E, et al: Anaplastic thyroid carcinoma. Cancer 103(7): 1330-1335, 2005.
14) Ha CS, et al: Localized non-Hodgkin lymphoma involving the thyroid gland. Cancer 91(4): 629-635, 2001.
15) Tsang RW, et al: Localized mucosa-associated lymphoid tissue lymphoma treated with radiation therapy has excellent clinical outcome. J Clin Oncol 21(22): 4157-4164, 2003.
16) 茂松直之ほか：有痛性骨転移に対する放射線治療の鎮痛効果. 日本医放会誌 55(9): 677 681, 1995.

Radiotherapy and Oncology 85 (2007) 443–449
www.thegreenjournal.com

Lung cancer SBRT

Differences in the definition of internal target volumes using slow CT alone or in combination with thin-slice CT under breath-holding conditions during the planning of stereotactic radiotherapy for lung cancer

Satoshi Seki[a], Etsuo Kunieda[a,*], Atsuya Takeda[b], Tomoaki Nagaoka[c], Hossain M. Deloar[d], Takatsugu Kawase[a], Junichi Fukada[a], Osamu Kawaguchi[a], Minoru Uematsu[a], Atsushi Kubo[a]

[a]*Department of Radiology, Keio University, Tokyo, Japan,* [b]*Department of Radiology, Ofuna Chuo Hospital, Kanagawa, Japan,* [c]*National Institutes of Information and Communications Technology, Japan,* [d]*Oncology Service, Medical Physics and Bioengineering Department, Christchurch Hospital, New Zealand*

Abstract

***Purpose*: To investigate how the delineations of the internal target volume (ITV) made from 'slow' CT alter with reference to 'thin-slice' CT.**

***Materials and methods*: Thin-slice CT images taken under breath-holding conditions and slow CT images taken under shallow-breathing conditions (8 s/image) of 11 lung cancers were used for this study. Five radiation oncologists delineated ITV of the 11 lesions using slow CT images (ITV1), and then redefined them with reference to thin-slice CT images (ITV2). SD-images (standard deviation image) were created for all patients from ITV images in order to visualize the regional variation of the ITVs.**

***Results*: The mean value of ITV2 was smaller than that initially defined by ITV1. There was no significant change in ITV1 and ITV2 between operators with regard to standard deviation in volume. There was a significant difference in the distribution of the ratio of ITV1 to ITV2 obtained on thin-slice CTs between cases with and without ground glass opacity. In cases without ground glass opacity there was a tendency for ITV2 to have a smaller volume than ITV1.**

***Conclusions*: Combined use of slow CT and thin-slice CT in delineation of ITV contours appeared to be useful in making adjustments for obscured tumor images caused by respiratory movement.**

Keywords: Stereotactic radiotherapy; Lung cancer; Target volume delineation; Slow CT

Stereotactic irradiation can deliver high radiation doses to localized lesions with great accuracy, allowing a strong anti-tumoral effect while lessening radiation injury to normal tissues. Although historically it has been applied to the treatment of small intracranial tumors with excellent results [1], its indications have been widened recently to include the treatment of lesions of the trunk [2–6]. Defining the extent of the area to be targeted is crucial for this treatment. Inadequate target volumes alter the dose distribution to the lesion, as well as to the surrounding normal tissues, and may therefore lead to inadequate therapeutic outcomes. For tumors of the trunk, such as lung cancer, target tumors move with the respiration-induced motion of the thorax or diaphragm [7].

If a large internal margin (IM) is defined, excessive doses of irradiation may be delivered to normal tissues. Conversely, if small internal target volume (ITV) is defined, potentially insufficient irradiation doses are delivered to the tumors, as tumor mobility may extend beyond the previously defined target region [8–10].

Although CT data acquired under breath-holding conditions can be used to visualize tumor shape, it cannot be used directly to determine the planning target volume, due to movement during the respiratory cycle or for other reasons. Even with CT images acquired under free breathing, limited tumor trajectory volumes can be detected if conventional short scanning times are used [11].

Four-dimensional CT (4D CT) has been used to investigate the motion of the anatomical structure and the tumor [12–16]. This technique is superior for detecting respiration-induced, three-dimensional motion of the tumor and will become the dominant technique in the near future [12–16]. However, it requires multi-detector low CT (MD-CT) as well as a device that can detect respiratory motion [17].

0167-8140/$ - see front matter doi:10.1016/j.radonc.2007.10.010

The visualization of respiration-induced tumor mobility has been attempted using CT scans taken with very long scan times per slice (slow CT) [18–20]. However, this technique can fail to visualize fine structures surrounding solid parts of the tumor [21]. There is a possibility that more precise definitions of target volumes could be achieved by combining thin-slice CT obtained under breath-holding conditions that are capable of visualizing fine tumor shape, and slow CT capable of visualizing the entire volume of the tumor trajectory. The purpose of our study was to investigate how the delineations of ITV made from slow CT alter with reference to thin-slice CT.

Materials and methods

Five experienced radiation oncologists were selected as operators for CT images from 11 patients with T1 to T3 lung cancer (mean tumor diameter = 2.8 ± 1.0 cm) who were scheduled to undergo hypofractionated stereotactic radiotherapy. The locations of the lesions are shown in Fig. 1. Thin-slice helical CT under conventional breath-holding conditions and slow CT under steady respiration were performed using a CT scanner (X-Vigour, Toshiba, Tokyo, Japan) on all 11 patients. Thin-slice CT scanning was conducted with a slice thickness of 2 mm (pitch 1:1, 120 kVp, and 200 mA) at 1 s per image under breath-holding conditions. Thin-slice CT series were taken for the target lesion and the adjacent range during a single breath-hold, with the inspiration levels being approximately the mid point of shallow inspiration and shallow expiration following training of shallow and regular respiration of the patients.

For slow CT scanning, patients were instructed to breathe shallowly. If fluoroscopic observation revealed that tumor mobility exceeded 1 cm in the cranio-caudal direction, a corset was used to inhibit movement of the abdominal wall and diaphragm. Slow CT scans were performed between 20 mm from the cranial and 20 mm from the caudal tumor edge, with a slice thickness of 2 mm, at 120 kVp and 400 mA. Scan time per image was 8 s, which was longer than the duration of one respiratory cycle.

Definition of target delineation

Each operator independently defined the target delineation from the CT images using the radiation therapy planning system (RTPS; XiO, CMS, St. Louis, Missouri). To avoid discrepancies in the appearance of ITV depending on different window levels, targets were delineated under the lung window setting with a window width of 2000 HU and window level of −700 HU for all experiments.

Delineation of ITV with slow CT alone (ITV1)

As the first step, the ITV outline image was delineated using slow CT (ITV1). No particular common guideline criteria were laid down at this point regarding the degree to which speculation, atelectasis and so on were to be included, with judgment instead being left to the discretion of each individual operator.

Second delineation of ITV with slow CT, while referring to thin-slice CT (ITV2)

Following the delineation of ITV1 as described above, ITV outline was delineated by using slow CT images once again. While simultaneously referring to thin-slice CT images taken under breath-holding conditions, the previously created ITV was modified with the aid of RTPS (ITV2).

The thin-slice CT images taken under breath-hold conditions were displayed on a computer display adjacent to the display of RTPS. During the delineation of ITV2, the operators were allowed to scroll both the displays when required.

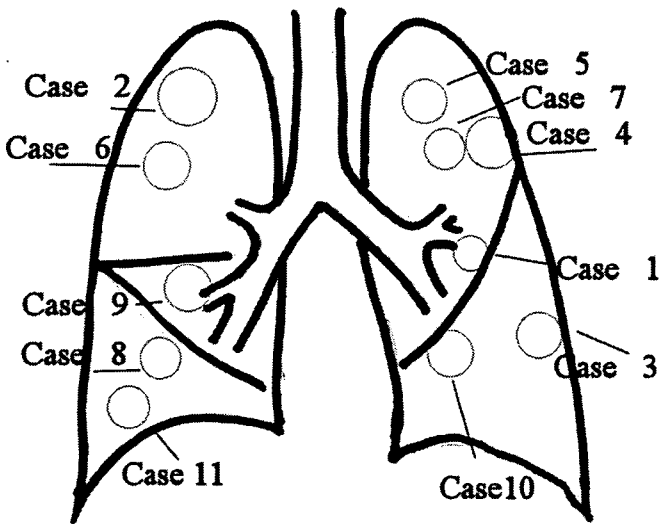

Fig. 1. Calculation of delineated target area and volume. Localizations of lung tumors in cases 1–11 are shown in the figure. The numbers of the circles indicate the case numbers. The position and size of each tumor are as follows. Case 1: lingula of left lung, T1 Φ2 cm, case 2: upper lobe of right lung, T3 Φ4 cm, case 3: lower lobe of left lung, T1 Φ2 cm, case 4: upper lobe of left lung, T2 Φ4 cm, case 5: upper lobe of left lung, T2 Φ3 cm, case 6: upper lobe of right lung, T2 Φ3 cm, case 7: upper lobe of left lung, T1 Φ2 cm, case 8: lower lobe of right lung, T2 Φ3 cm, case 9: middle lobe of right lung, T3 Φ3 cm, case 10: lower lobe of left lung, T2 Φ3 cm, case 11: lower lobe of right lung, T1 Φ2 cm.

The slice positions of both the breath-holding CT and slow CT may not correspond with each other, as the inspiration level of the former CT series was not necessarily totally reproducible or stable. Therefore, adjustments of the two CT series were made according to the view of the operators, based on careful observation of the detailed morphological characteristics of the lesion and other structures such as vessels or bronchi.

The number of pixels included inside the ITV1 delineations was counted to obtain the tumor area for each slice. The ITV1 was then calculated from the sum of the areas multiplied by the slice thickness. ITV2 was calculated in the same way.

Statistical images

To visualize the differences in individual target definitions between operators, the extent of target delineation was statistically analyzed pixel by pixel. Prior to statistical analysis, contour shapes were converted to binary images by replacing each pixel inside and outside the delineated area with pixel values 1 and 0, respectively.

The standard deviation (SD) of each pixel was then calculated using the formula shown below. Statistical images for ITV1 and ITV2 were generated from the binary images of all patients using the programming language Matlab (Ver. 2006a, The MathWorks, Inc., Natick, MA, USA).

SD-image (standard deviation image):

Pixel value: $\sigma = \frac{1}{N}\sum_{i=1}^{N}(Z_i - \mu)$

N: number of operators;
i: operator;
Z_i: pixel value of operator i for the corresponding pixel;
μ: mean of pixel values obtained by all operators.

Results

Comparison of ITV

The mean and standard deviation of ITVs amongst all operators for each case are shown in Table 1. The ratio of ITV2 to ITV1 was used in order to examine the changes between ITV1 defined with slow CT alone, and ITV2, which is a modification of ITV1 with reference to thin-slice CT.

Table 1
Mean volume

	ITV1	ITV2	ITV2/ITV1	GGO
Case 1	2.9 ± 1.4	3.0 ± 2.0	1.03 ± 0.20	(+)
Case 2	46.2 ± 7.5	35.6 ± 4.3	0.77 ± 0.09	(−)
Case 3	3.9 ± 0.4	4.2 ± 1.2	1.06 ± 0.24	(+)
Case 4	48.2 ± 6.0	47.1 ± 4.9	0.98 ± 0.02	(+)
Case 5	11.3 ± 2.5	11.5 ± 4.6	1.02 ± 0.27	(+)
Case 6	17.2 ± 1.5	15.4 ± 1.5	0.90 ± 0.04	(−)
Case 7	8.0 ± 2.9	6.0 ± 1.6	0.74 ± 0.19	(−)
Case 8	16.4 ± 4.4	12.7 ± 3.6	0.78 ± 0.27	(−)
Case 9	21.1 ± 5.4	17.0 ± 3.5	0.80 ± 0.24	(+)
Case 10	11.2 ± 3.2	8.6 ± 3.2	0.77 ± 0.12	(−)
Case 11	25.4 ± 8.9	18.7 ± 9.4	0.73 ± 0.28	(−)

ITV, internal target volume; GGO, ground glass opacity; ITV1, ITV delineated using slow CT only; ITV2, ITV delineated using slow CT images, referring to breath-holding thin-slice CT.

The ITVs were compared by two-way analysis of variance (ANOVA) to estimate the effect of the ITV delineation among operators and cases. While there was no significant difference between the five operators for the size of ITV delineations, there was a significant difference between ITV1 and ITV2 volumes ($p < 0.01$). The ITV2 volumes were on average 18% smaller than the ITV1 volumes (Table 1).

A radiologist (S.S.) independently evaluated each case and categorized them into those with ground glass opacity in the surrounding area of the tumor and those without ground glass opacity (Fig. 2). The definitions of ground glass opacity were made using thin-slice breath-hold CT. There was a significant difference in the ratio of ITV2 to ITV1 between the cases with and without ground glass opacity (Fig. 3). That is, there were no evident decreases in target

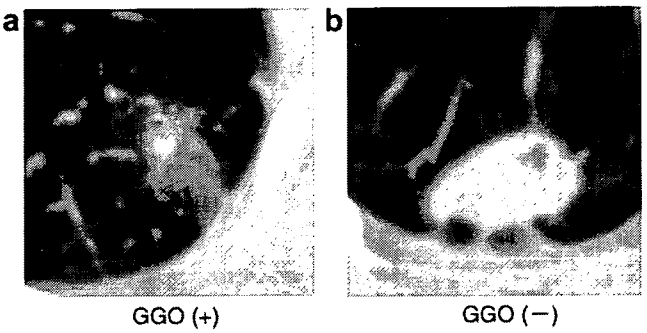

Fig. 2. Example of a case with ground glass opacity (a), and a case without ground glass opacity (b).

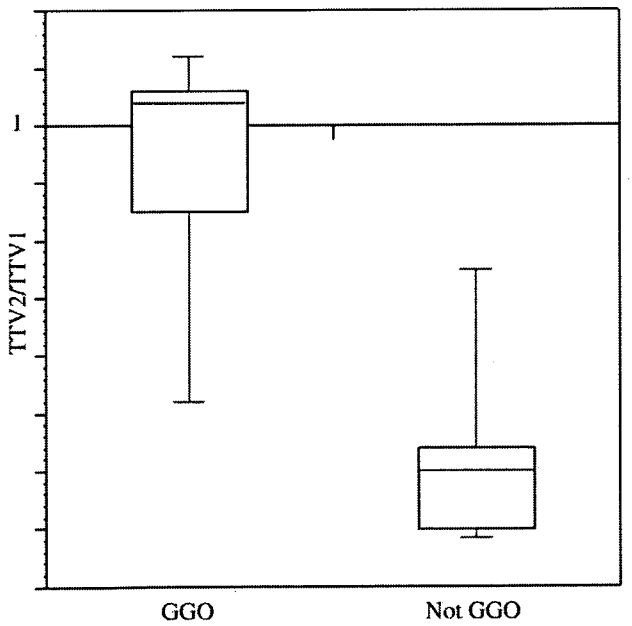

Fig. 3. The distribution of the ratio of ITV2 to ITV1 between the cases with and without ground glass opacity. There was a clear tendency for smaller ratio of ITV2 to ITV1 in cases without ground glass opacity than in cases with ground glass opacity.

volume when the operators refer to thin-slice CT in cases with ground glass opacity.

We performed more detailed analyses of target delineations by means of SD-images (Figs. 4 and 5). Although there were differences in the area of tumor delineation between ITV2 and ITV1 in many cases, relatively small changes in the distribution pattern of SD values were observed. The analyses indicated that there were some cases in which the reference to thin-slice CT images had influenced the target outline recognition (Fig. 5). In this case (case 10), the structure seen as a spiculation on the left lower site of the tumor shown on the slow CT image corresponded to the region with high SD values for ITV1. A higher value meant there was a greater degree of inconsistency between the decisions of the operators as to whether or not the area should have been included in the ITV. The regions with high SD values for ITV1 were excluded from the target delineations by the operators in ITV2 (in which thin-slice CT of the same position was considered). The thin-slice CT apparently revealed this region to be a part of the bronchi. Table 2 shows the

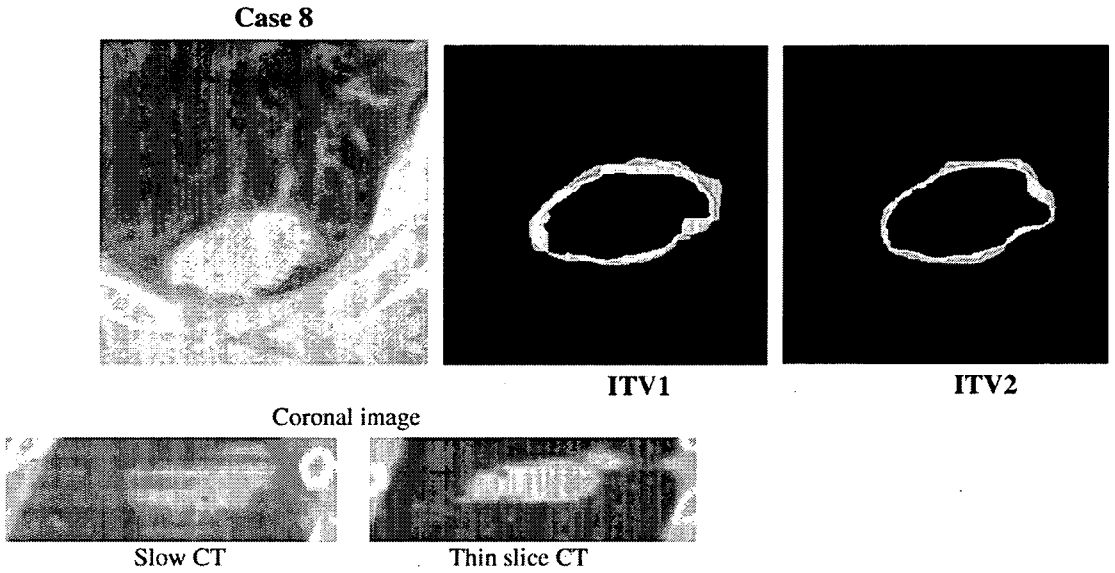

Fig. 4. SD-image (ITV1, ITV2) for case 8. Highest pixel SD values are shown in yellow, followed by green, and blue in descending order. The central part of the target (shown as black) means that all operators recognized it as the target volume. The outer part of the target (also shown as black) means that no operators recognized it as the target volume.

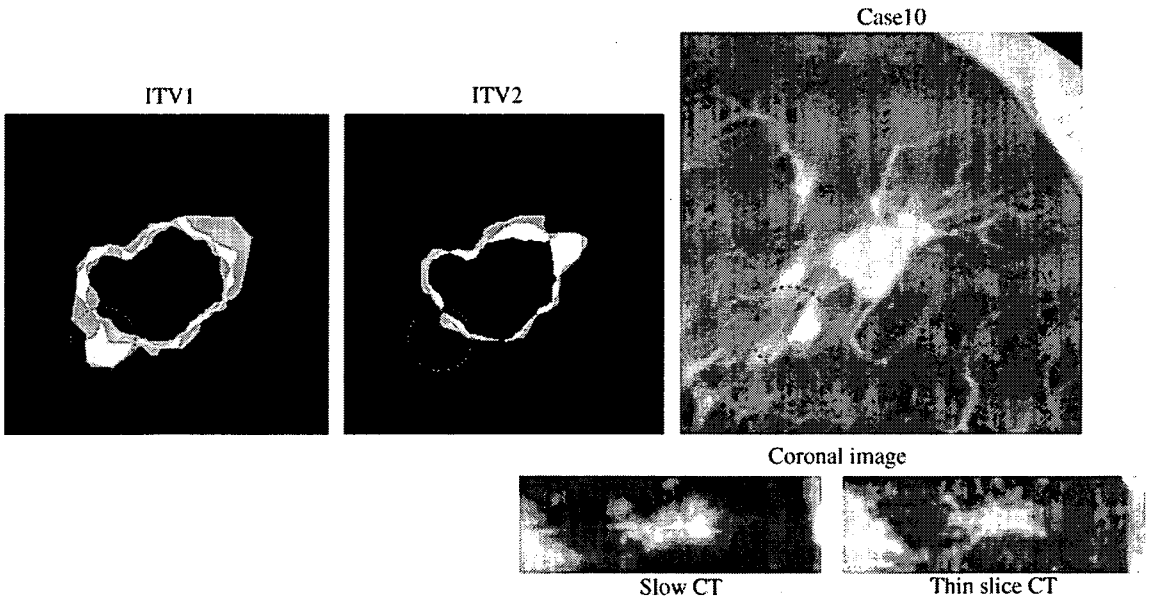

Fig. 5. SD-image (ITV1, ITV2) for case 11. The regions with high SD values for ITV1 were excluded from the target delineations by the operators in ITV2. The thin-slice CT apparently revealed this region to be a part of the bronchi.

Table 2
Volumes that all operators recognized as the internal target volume

	ITVc1	ITVc2	ITVc1/ITV1	ITVc2/ITV2
Case 1	1.3	1.1	0.47	0.38
Case 2	28.7	23.6	0.62	0.66
Case 3	2.9	2.4	0.73	0.57
Case 4	37.2	34.7	0.77	0.74
Case 5	6.9	6.2	0.61	0.54
Case 6	12.1	11.0	0.71	0.72
Case 7	4.4	3.7	0.55	0.63
Case 8	8.7	8.4	0.53	0.66
Case 9	11.7	11.1	0.55	0.65
Case 10	5.3	5.1	0.48	0.60
Case 11	12.1	7.0	0.48	0.38

ITVc, the volume that all operators recognized as the internal target volume; ITVc1, ITVc delineated using slow CT only; ITVc2, ITVc delineated using slow CT images, referring to breath-holding thin-slice CT.

volumes that all the operators judged as the target volume, ITVc1 or ITVc2 (i.e., the union of all target volumes determined by operators) in each case.

Discussion

To minimize the effect of respiratory motion, stereotactic radiotherapy for lesions of the trunk has been conducted using various techniques, including breath-holding [22,23], respiratory-gated tracking [24,25] and real-time tumor tracking [26,27]. The ICRU (International Commission on Radiation Units and measurements) report 62 [28] proposed a definition for four tumor volumes, gross tumor volume (GTV), clinical target volume (CTV), internal target volume (ITV), and planning target volume (PTV). The term ITV was adopted into the ICRU-62 report and was taken to represent the CTV plus the Internal Margin (IM), and was intended to compensate for movement and variation in site, size, and shape of organs and tissues contained within or adjacent to the CTV. In a review article in 2004, Purdy discussed some of the limitations and potential pitfalls of the recommendations contained in the current ICRU Reports 50 and 62, particularly in regard to issues of organ motion [29].

Free breathing irradiation

Although the planning target volumes tend to be larger, irradiation under free breathing is a simple and reliable method, which can be performed without the need for special equipment to detect respiratory motion, providing that appropriate internal margins are used. However, the question of how to determine these internal margins remains a difficult problem [29,30]. If large margins are used, then the irradiation volume increases, resulting in excessive radiation exposure to normal tissues. However, if small margins are used, then it becomes unlikely that the periphery of the target will receive a sufficient radiation dose. More sophisticated margin recipes to create the PTV have been proposed by several investigators [31,32].

While fluoroscopy-based observation of the tumor trajectory is another possible approach to define the margin, margins based on fluoroscopically two-dimensional tumor trajectories may not adequately cover substantial tumor mobility, as tumor motion associated with respiration occurs not only in the cranio-caudal direction but also in the antero-posterior direction.

4D CT

4D CT (acquisition of a sequence of CT image sets over consecutive segments of a breathing cycle) [12] is able to demonstrate both respiratory and cardiac motion and has been applied to the treatment planning of radiotherapy. 4D CT can provide three-dimensional data on tumor position at several points during the breathing cycle, with a somewhat reduced temporal resolution compared to conventional CT, thus providing a compromise between the high-quality time resolution of a fluoroscopic study and the detailed 3D information of a CT scan. Although it requires dedicated devices with which conventional radiotherapy departments are not commonly equipped, this technique has a fundamental advantage in terms of detecting tumor motion [33].

Slow CT

Lagerwaard et al. used a slow CT technique with a scanning time of 4 s per slice, in addition to conventional CT for radiotherapy planning, in an attempt to generate more accurate target volumes during shallow respiration. Based on the images obtained, they reported being able to define target volumes with high reproducibility and reliability without the need for specialized equipment [34,35]. De Koste et al. analyzed seven lung tumors located in the lower lobes, which is the most mobile location [35]. They showed that slow CT scans generated larger and more reproducible target volumes than rapid planning scans. They proposed PTVs derived from a single slow CT scan plus a 5-mm margin to represent the "optimal" PTV, and concluded that a full rapid scan of the entire thorax and a limited slow scan were necessary for treatment planning in patients with peripheral lung cancers. Wurstbauer et al. reported that the use of slow CT enabled the drawing of tighter margins in the planning of external beam treatment for lung cancer [36].

Takeda et al. also performed slow CT at a rate of 8 s per slice in order to define an optimal ITV that included the entire tumor trajectory volume [21]. However, these scanning strategies were devised to visualize the average density of the anatomical structures in the tumor trajectory, and therefore that movement during a long scanning time can lead to obscure images of the tumor and adjacent anatomical structures such as bronchi or vessels. Thus, slow CT is generally thought to be unable to visualize complicated tumors or areas of fine spiculation, consolidation, or emphysematous changes with any degree of accuracy, which suggests that optimal ITV definition may not always be possible with the use of slow CT alone.

Based on target tumor delineation, differences between the spatial distribution of ITV1 and ITV2 were assessed to investigate the impact on ITV delineation of referring to thin-slice CT under breath-holding conditions.

A comparison of the volumes of ITV delineated with slow CT alone, and ITV determined using thin-slice CT showed that the latter was smaller with regard to target volume overall. It is thought that this is related to blurring of the image, which occurs with slow CT under free breathing conditions, due to the respiration-induced motion effect of the tumor, thorax, bronchus and blood vessels. The outline of the tumor periphery cannot be visualized clearly with slow CT. Differentiation of normal structures (i.e., blood vessels, etc.) from tumors was often impossible. It is assumed that wider target delineations were preferred by the operators during the ITV1 definitions, in order to avoid a situation in which the tumor was no longer included in the target volume.

By referring to breath-holding CT images, the detailed structure of the tumor periphery can be visualized with increased clarity. It is thought that operators were able to recognize structures, within the region indistinct with slow CT, that do not need to be included as part of the target volume.

On the other hand, there were also cases in which ITV2 became larger than ITV1, such as in cases 1, 3 and 5. By examining the characteristics of the images in cases such as these, we were able to conclude that when a large amount of ground glass opacity was included within the tumor there was a tendency for ITV2 to be larger than ITV1, or for it not to get smaller.

It would be fair to say that by referring to thin-slice CT, there is a possibility that ITV may be delineated as smaller than necessary. However, creating a standard that would serve as the "correct way" to carry out ITV delineation is an extremely difficult and almost unsolvable problem. For this reason, this study did not fully examine the question as to whether or not the change corresponded to the "real" lesion confirmed by pathological findings. However, this study indicated there was a tendency for ITV2 to have a smaller volume than ITV1, especially in cases without ground glass opacity.

Breath-hold CT is considered to be a standard for target delineation for small lung tumors because of its ability to show detailed structures if internal margins and reproducibility of the target position are not taken into account. On the other hand, slow CT has superior reproducibility for target positioning and detecting the range of interfractional motion.

Using thin-slice breath-hold CT as a planning CT may cause systemic errors in target positioning, as the inspiration level at breath-hold is not always reproducible [32]. However, our proposed technique uses thin-slice breath-hold CT as a reference for observing the detailed structure of the tumor peripheral and does not use it as a reference for the "position" of the tumor. For these reasons, we consider it reasonable to use breath-hold CT with slow CT for treatment planning of small lung lesions.

Regarding the standard deviation (SD) of target volume of all the operators, there was no tendency towards a clear increase or decrease between the SDs for ITV1 and ITV2. In other words, referring thin slice, high-resolution CT did not improve the variation in target volume recognition between the operators.

The regional analyses with SD-images indicated that there were some cases in which the reference to thin-slice CT images influenced target outline recognition (Fig. 5). Trying to determine the proportion of actual tumor from the opacity visualized in the original CT image is fraught with great difficulty, and it is not possible to prepare a standard outline delineation. It is thought that the variation observed among operators is due to uncertainty regarding outline delineation. Although it is necessary to make comparisons with more detailed pathological findings in order to eliminate variation among operators, such comparisons fall outside the scope of this study.

While there is no fixed standard for GTV delineation among radiation oncologists, reference to thin-slice CT images may be a useful strategy to correct information in images that are unclear due to respiratory movement, thereby improving the accuracy of ITV description.

Positron emission tomography (PET) or single photon emission tomography (SPECT) is usually performed with longer data acquisition time than CT. Therefore, these techniques may provide a more accurate representation of the GTV encompassing motion of such tumors and therefore have the potential to provide patient-specific motion volumes for an individualized ITV [29]. However, to date the resolution of PET and SPECT may be insufficient for delineating small lung lesions without using CT. Future development of these modalities may widen their application for delineating small lung lesions.

Conclusion

We compared target delineation for lung tumors with slow CT alone, and then with slow CT and high-resolution thin-slice CT. Standard deviation images were created from the delineations of each operator in order to analyze the inter-operator differences for individual structures. The use of slow CT images together with thin-slice CT would be a useful technique for achieving more elaborate treatment plans concerning fine structures in the tumor peripheral area. With slow CT alone, there is a possibility that tiny lesions in the tumor area or ground glass opacities may be delineated inaccurately. Furthermore, there is a tendency to erroneously incorporate surrounding structures such as blood vessels in the target volume.

Acknowledgment

This work was supported by a Grant-in-Aid for Scientific Research from The Japan Society for the Promotion of Science (JSPS).

* **Corresponding author. Etsuo Kunieda**, Department of Radiology, Keio University, 35 Shinanomachi, Shinjuku, Tokyo 160-8582. Japan. *E-mail address:* kunieda-mi@umin.ac.jp

Received 2 July 2007; received in revised form 24 September 2007; accepted 6 October 2007; Available online 5 November 2007

References

[1] Langer CJ, Mehta MP. Current management of brain metastases, with a focus on systemic options. J Clin Oncol 2005;23:6207–19.

[2] Zimmermann FB, Geinitz H, Schill S, et al. Stereotactic hypofractionated radiation therapy for stage I non-small cell lung cancer. Lung Cancer 2005;48:107–14.

[3] Nagata Y, Takayama K, Matsuo Y, et al. Clinical outcomes of a phase I/II study of 48 Gy of stereotactic body radiotherapy in 4 fractions for primary lung cancer using a stereotactic body frame. Int J Radiat Oncol Biol Phys 2005;63:1427–31.
[4] McGarry RC, Papiez L, Williams M, Whitford T, Timmerman RD. Stereotactic body radiation therapy of early-stage non-small-cell lung carcinoma: phase I study. Int J Radiat Oncol Biol Phys 2005;63:1010–5.
[5] Timmerman R, McGarry R, Yiannoutsos C, et al. Excessive toxicity when treating central tumors in a phase II study of stereotactic body radiation therapy for medically inoperable early-stage lung cancer. J Clin Oncol 2006;24:4833–9.
[6] Kavanagh BD, McGarry RC, Timmerman RD. Extracranial radiosurgery (stereotactic body radiation therapy) for oligometastases. Semin Radiat Oncol 2006;16:77–84.
[7] Keall PJ, Mageras GS, Balter JM, et al. The management of respiratory motion in radiation oncology report of AAPM Task Group 76. Med Phys 2006;33:3874–900.
[8] Seppenwoolde Y, Shirato H, Kitamura K, et al. Precise and real-time measurement of 3D tumor motion in lung due to breathing and heartbeat, measured during radiotherapy. Int J Radiat Oncol Biol Phys 2002;53:822–34.
[9] van Sornsen de Koste JR, Lagerwaard FJ, Nijssen-Visser MR, Graveland WJ, Senan S. Tumor location cannot predict the mobility of lung tumors: a 3D analysis of data generated from multiple CT scans. Int J Radiat Oncol Biol Phys 2003;56:348–54.
[10] Shimizu S, Shirato H, Kagei K, et al. Impact of respiratory movement on the computed tomographic images of small lung tumors in three-dimensional (3D) radiotherapy. Int J Radiat Oncol Biol Phys 2000;46:1127–33.
[11] Balter JM, Ten Haken RK, Lawrence TS, Lam KL, Robertson JM. Uncertainties in CT-based radiation therapy treatment planning associated with patient breathing. Int J Radiat Oncol Biol Phys 1996;36:167–74.
[12] Keall P. 4-dimensional computed tomography imaging and treatment planning. Semin Radiat Oncol 2004;14:81–90.
[13] Ichikawa T, Kumazaki T. 4D-CT: a new development in three-dimensional hepatic computed tomography. J Nippon Med Sch 2000;67:24–7.
[14] Ford EC, Mageras GS, Yorke E, Ling CC. Respiration-correlated spiral CT: a method of measuring respiratory-induced anatomic motion for radiation treatment planning. Med Phys 2003;30:88–97.
[15] Vedam SS, Keall PJ, Kini VR, Mostafavi H, Shukla HP, Mohan R. Acquiring a four-dimensional computed tomography dataset using an external respiratory signal. Phys Med Biol 2003;48:45–62.
[16] Rietzel E, Chen GT, Choi NC, Willet CG. Four-dimensional image-based treatment planning: target volume segmentation and dose calculation in the presence of respiratory motion. Int J Radiat Oncol Biol Phys 2005;61:1535–50.
[17] Stock M, Kontrisova K, Dieckmann K, Bogner J, Poetter R, Georg D. Development and application of a real-time monitoring and feedback system for deep inspiration breath hold based on external marker tracking. Med Phys 2006;33:2868–77.
[18] Underberg RW, Lagerwaard FJ, Slotman BJ, Cuijpers JP, Senan S. Benefit of respiration-gated stereotactic radiotherapy for stage I lung cancer: an analysis of 4DCT datasets. Int J Radiat Oncol Biol Phys 2005;62:554–60.
[19] Slotman BJ, Lagerwaard FJ, Senan S. 4D imaging for target definition in stereotactic radiotherapy for lung cancer. Acta Oncol 2006;45:966–72.
[20] Guckenberger M, Wilbert J, Krieger T, et al. Four-dimensional treatment planning for stereotactic body radiotherapy. Int J Radiat Oncol Biol Phys 2007;69:276–85.
[21] Takeda A, Kunieda E, Shigematsu N, et al. Small lung tumors: long-scan-time CT for planning of hypofractionated stereotactic radiation therapy – initial findings. Radiology 2005;237:295–300.
[22] Onishi H, Kuriyama K, Komiyama T, et al. CT evaluation of patient deep inspiration self-breath-holding: how precisely can patients reproduce the tumor position in the absence of respiratory monitoring devices? Med Phys 2003;30:1183–7.
[23] Mageras GS, Yorke E. Deep inspiration breath hold and respiratory gating strategies for reducing organ motion in radiation treatment. Semin Radiat Oncol 2004;14:65–75.
[24] Kubo HD, Hill BC. Respiration gated radiotherapy treatment: a technical study. Phys Med Biol 1996;41:83–91.
[25] Berson AM, Emery R, Rodriguez L, et al. Clinical experience using respiratory gated radiation therapy: comparison of free-breathing and breath-hold techniques. Int J Radiat Oncol Biol Phys 2004;60:419–26.
[26] Shirato H, Shimizu S, Shimizu T, Nishioka T, Miyasaka K. Real-time tumour-tracking radiotherapy. Lancet 1999;353:1331–2.
[27] Shimizu S, Shirato H, Kitamura K, et al. Use of an implanted marker and real-time tracking of the marker for the positioning of prostate and bladder cancers. Int J Radiat Oncol Biol Phys 2000;48:1591–7.
[28] ICRU report 62: Prescribing, recording and reporting photon beam therapy. Bethesda: International Commission on Radiation Units and Measurements, 1999.
[29] Purdy JA. Current ICRU definitions of volumes: limitations and future directions. Semin Radiat Oncol 2004;14:27–40.
[30] Shirato H, Seppenwoolde Y, Kitamura K, Onimura R, Shimizu S. Intrafractional tumor motion: lung and liver. Semin Radiat Oncol 2004;14:10–8.
[31] Craig T, Battista J, Moiseenko V, Van Dyk J. Considerations for the implementation of target volume protocols in radiation therapy. Int J Radiat Oncol Biol Phys 2001;49:241–50.
[32] van Herk M. Errors and margins in radiotherapy. Semin Radiat Oncol 2004;14:52–64.
[33] Rietzel E, Liu AK, Doppke KP, et al. Design of 4D treatment planning target volumes. Int J Radiat Oncol Biol Phys 2006;66:287–95.
[34] Lagerwaard FJ, Van Sornsen de Koste JR, Nijssen-Visser MR, et al. Multiple "slow" CT scans for incorporating lung tumor mobility in radiotherapy planning. Int J Radiat Oncol Biol Phys 2001;51:932–7.
[35] de Koste JR, Lagerwaard FJ, de Boer HC, Nijssen-Visser MR, Senan S. Are multiple CT scans required for planning curative radiotherapy in lung tumors of the lower lobe? Int J Radiat Oncol Biol Phys 2003;55:1394–9.
[36] Wurstbauer K, Deutschmann H, Kopp P, Sedlmayer F. Radiotherapy planning for lung cancer: slow CTs allow the drawing of tighter margins. Radiother Oncol 2005;75:165–70.

Physica Medica (2008) xx, 1–8

available at www.sciencedirect.com

ScienceDirect

journal homepage: http://intl.elsevierhealth.com/journals/ejmp

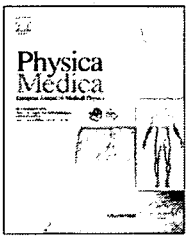

ORIGINAL PAPER

Variation of dose distribution of stereotactic radiotherapy for small-volume lung tumors under different respiratory conditions

E. Kunieda [a,*], H.M. Deloar [b], N. Kishitani [c], T. Fujisaki [c], T. Kawase [a], S. Seki [a], Y. Oku [a], A. Kubo [a]

[a] *Department of Radiation Oncology, Keio University, Tokyo, Japan*
[b] *Department of Medical Physics and Bioengineering, Christchurch Hospital, Christchurch, New Zealand*
[c] *Department of Radiological Sciences, Ibaraki Prefectural University of Health Sciences, Ibaraki, Japan*

Received 4 July 2007; received in revised form 6 February 2008; accepted 8 February 2008

KEYWORDS
Stereotactic radiotherapy;
Lung tumor;
Path-length;
Electron density

Abstract *Purpose:* To clarify the effects of respiratory condition on dose calculation for stereotactic radiotherapy of small lung tumors.
Methods and materials: Computed tomography (CT) data were obtained for nine tumors (diameter, 2.1–3.6 cm; mean, 2.7 cm) during the stable state, deep expiration, and deep inspiration breath-hold states. Rotational Irradiation with 3 non-coplanar arcs (Rotational Irradiation) and static irradiation with 18 non-coplanar ports (Static Irradiation) using 6-MV photons were evaluated using Fast Fourier Transform (FFT) convolution and Multigrid (MG) superposition algorithms. Dose-volume histograms (DVHs), mean path-length (PL) and mean effective path-length (EPL) were calculated.
Results: Although the PL was larger for the inspiration state than for the stable state and the expiration state, the EPL was 0.4–0.5 cm smaller in the inspiration state than in the expiration state ($p = 0.01$ for Rotational Irradiation; $p = 0.03$ for Static Irradiation). The isocenter dose obtained by the FFT convolution algorithm was 7–12% higher than that obtained with the MG superposition algorithm. A leftward shift of the DVH obtained by MG superposition was noted for the inspiration state compared with the expiration state.
Conclusions: The choice of the proper algorithm is important to accounting for changes in respiration state. Differences in isocenter dose were not large among the respiratory states

* Corresponding author: Department of Radiation Oncology, Keio University, 35 Shinanomachi, Shinjuku, Tokyo 160-8582, Japan. Tel.: +81 3 3353 1211x62531; fax: +81 3 3359 7425.
E-mail address: kunieda-mi@umin.ac.jp (E. Kunieda).

1120-1797/$ - see front matter © 2008 Published by Elsevier Ltd on behalf of Associazione Italiana di Fisica Medica.
doi:10.1016/j.ejmp.2008.02.002

Please cite this article in press as: Kunieda E et al., Variation of dose distribution of stereotactic radiotherapy for small-volume lung tumors under different respiratory conditions, Physica Medica (2008), doi:10.1016/j.ejmp.2008.02.002

analyzed. EPL was a little shorter for inspiration than for expiration, although there were larger and reverse trends in path length. A leftward shift of the DVH obtained for the inspiration state when MG superposition was used.

Introduction

Stereotactic radiotherapy (SRT) is currently performed to treat small tumors of the trunk [1,2]. In particular, SRT has gained acceptance as an effective means of treatment for lung tumors [3–5]. However, factors such as the presence of inhomogeneous density within the chest, respiratory motion, and lack of lateral electron equilibrium due to a small radiation field may have an effect on the accuracy of the dose calculation for lung SRT performed with an X-ray computed tomography (CT)-based radiation treatment planning system (RTPS) [5,6].

CT scans for SRT planning for lung tumors are often obtained with deep-inspiration breath hold or other breath-hold techniques. To estimate the mean position and range of tumor motion during respiratory cycles, CT scans during free breathing, called "slow CT," are often used [7–10]. A pair of inhalation and exhalation breath-hold CT scans, and four-dimensional CT [11–13] are able to indicate the range of the tumor motion without the blurring effect caused by slow CT. These techniques were well summarized in a report from the American Association of Physicists in Medicine (AAPM) Task Group 76 [14]. However, based on respiratory conditions, variations in lung densities will cause changes in the mean path-length (PL), mean effective path-length (EPL), and energy distributions in the medium and finally bring about a change the density-scaling factor, which is used to correct the inhomogeneity correction.

This study was designed to clarify the effects of respiratory condition on dose distribution using convolution and superposition algorithms [15,16] in SRT for small lung tumors. To determine the range of variations, we evaluated path-length and effective path-length data under extreme breathing conditions (i.e. deep-expiration, and deep-inspiration breath-hold) as well as stable-state breath-hold conditions. Dose distributions were obtained for rotation and multiple static-port irradiation, based on CT images of patients who were scheduled to undergo lung SRT. Furthermore, we investigated changes in dose distribution in the breathing conditions to determine the degree of influence on the dose calculation using clinical algorithms.

Methods

CT images

A total of 9 lung tumors (diameter range, 2.1–3.6 cm; mean, 2.7 cm) from 9 patients diagnosed with early-stage lung cancer (4 men, 5 women; mean age, 70 years) were evaluated. The cases used for this study were selected from consecutive patients treated with SRT for their lung lesions who agreed to be enrolled in this study. The approximate positions of the lesions are indicated in Fig. 1. CT scanning procedures in three breathing conditions and the use of data for this analysis were approved by the Institutional Review Board. Written informed consent was obtained from each participant prior to the CT scans after the purpose of the study had been fully explained.

Whole lungs including tumors were scanned using a multi-detector row (16 rows) helical CT (MDCT) (Aquilion; Toshiba Medical Systems Co., Ltd., Tokyo, Japan). A stereotactic body frame (Elekta AB, Stockholm, Sweden) was used for patient fixation, As a routine procedure for the planning of stereotactic radiotherapy, a series of breath-hold scans were carried out at approximately the mid-point of inhalation and expiration in the stable respiratory cycle (stable-state breath-hold). A series of slow CT scans during stable respiration for the tumor and the adjacent area was carried out to take the tumor motion into account. In addition, for those patients who agreed to take part in this study on a voluntary basis, two series of CT were performed for the whole lung under deep expiration breath-hold and deep inspiration breath-hold conditions. These three-phase breath-hold CT series were used for the following analysis. The breath-hold CT scans were obtained using 0.5 s/rotation, a helical pitch of 5.5, 2-mm thickness, and 7-mm thickness reconstruction with exposure conditions of 120 kV and 200 mA.

Treatment planning

CT data were transferred to 3D-RTPS (XiO version 2.4.0, CMS Co., St. Louis, Missouri, USA) via DICOM protocol from the CT scanner. CT data for stable-state breath-hold were used for treatment planning of the actual treatment.

Body contours, both lungs, and gross target volume (GTV) were delineated on each of the three-phase CT images by a radiation oncologist. The GTV was first created on stable-state breath-hold CT images and the delineation was then copied manually to the expiration and inspiration breath-hold images to follow the tumor motion. The isocenters were placed at the center of the GTV for each breath-hold CT series. A window width of 1500, and a window level of −700 were used to determine the GTV. Clinical target volume (CTV) was the same as the GTV and a 0.5 cm margin was added to the CTV in all directions in order to create the planning target volume (PTV).

For this experimental study, despite whatever technique was actually used for treatment, we adopted Rotational Irradiation with 3 non-coplanar arcs (−30°, 0°, +30° couch angle; 220° gantry arc on the lesion side) as shown in Fig. 2a (Rotational Irradiation) and Static Irradiation with 18 non-coplanar ports (−30°, 0°, +30° couch angle; 0°, 30°, 150°, 180°, 210°, 330° gantry angle on the lesion side) as shown in Fig. 2b (Static Irradiation). In all cases an additional 0.5 cm field margin was added to the PTV to generate a rectangular field size. Although the PTV sizes were

Please cite this article in press as: Kunieda E et al., Variation of dose distribution of stereotactic radiotherapy for small-volume lung tumors under different respiratory conditions, Physica Medica (2008), doi:10.1016/j.ejmp.2008.02.002